ELSEVIER

Contents lists available at ScienceDirect

Materials Today Communications

journal homepage: www.elsevier.com/locate/mtcomm





Statistical approach to optimize crashworthiness of thermoplastic commingled composites

Ricardo Mello Di Benedetto ^{a,b,*}, Guilherme Ferreira Gomes ^c, Anderson Janotti ^b, Antonio Carlos Ancelotti Junior ^c, Edson Cocchieri Botelho ^a

- a Materials and Technology Department, School of Engineering, São Paulo State University UNESP, Av. Ariberto Pereira da Cunha, 333,Guaratinguetá, SP, Brazil
- ^b Department of Materials Science & Engineering, University of Delaware UDEL, 212 DuPont Hall, Newark, DE, USA
- c Institute of Mechanical Engineering, Federal University of Itajubá UNIFEI, NTC Composite Technology Center, Av. BPS, 1303, Itajubá, MG, Brazil

ARTICLE INFO

Keywords:
High-performance composites
Crashworthiness
DOE
Commingled composites

ABSTRACT

A design of experiments analysis was developed to relate the processing conditions to the impact energy absorption capability of thermoplastic commingled composites. Based on low velocity impact test responses and statistical modeling, a factorial design was implemented to investigate the interaction of processing parameters with the polymer viscosity. The influence of thermal consolidation on materials performances were evaluated and quantified. The dataset was obtained according to the impact energy capability of carbon fiber/polyamide and carbon fiber/poly (ether-ether-ketone) commingled composites. The results identified the best combination of variables which improves crashworthiness of structural composites and leads to high impact energy absorption capabilities. The results revealed that the commingled composites crashworthiness strongly depends on the polymer yarn dispersion in the carbon fiber tow, that was identified and classified in different distribution patterns. This work represents a significant step towards manufacturing of thermoplastics composites with target structural performance.

1. Introduction

Structural polymer/carbon-fiber composite materials are of great interest to the automotive industry, potentially impacting weight and collision resistance of hybrid, plug-in hybrid and fully electric vehicles [1]. One of the main parameters/properties for such applications is the crashworthiness [2–4]. The human safety in eventual automotive crash or accident depends on improvements in impact energy absorption (*IEA*) capability of these composite materials. A review of recent literature points to research on this subject.

Koerich et al. (2014) [5] evaluated carbon fiber/polyamide and glass fiber/polyamide composite beams for use as automotive bumper subsystem. The authors used hot melt adhesive to compare beams performances and crashworthiness. The use of adhesives reduces the peak load of tests and the energy absorption improvement of the component. However, the study did not investigate the effect of thermal processing on the material performance.

The IEA capability of polymer/carbon-fiber composite structures, in

turn, depends on a large set of parameters in the thermal consolidation process which, together with the thermal properties of the polymeric matrix, directly affect performance. Di Benedetto et al. (2017) [6] proved that thermo-oxidative degradation affects the energy absorption capability of thermoplastic commingled composites. Low velocity impact tests (LVI) and compression after impact tests (CAI) were conducted and, according to the results of the study, crashworthiness is impaired by thermo-oxidative degradation of the polymeric matrix. Parina et al. (2010) [7] present a literature review of poly(ether ether ketone) (PEEK) degradation and flammability. Each stage of PEEK decomposition was investigated to detect and identify how degradation mechanisms occur. Although the results are expressive, the influence of processing parameters on energy absorption capability of thermoplastic composites should be more explored and related to processing optimization.

The study developed by Ren et al. [8] simulated the axial crushing of composite beams by a progressive failure model. The energy absorption was compared to experimental results from previous publications and

E-mail address: ricardob@udel.edu (R.M. Di Benedetto).

^{*} Corresponding author at: Materials and Technology Department, School of Engineering, São Paulo State University – UNESP, Av. Ariberto Pereira da Cunha, 333, Guaratinguetá, SP, Brazil.

literature data. The fiber strength and the friction coefficients affect *IEA* capability of composite materials. Garner and Adams [3] have already investigated these effects, and their study also revealed that the loading rate and the friction coefficients affect *IEA* and crashworthiness of the composite structure. The results were also compared to the work of Thornton [9] which the energy absorbed during the axial collapse of different composites were defined. The results of the studies correlated to specific interlaminar shear stress to the energy absorption capability of composite materials. Indeed, the shear properties have high influence on IEA, but it is important to understand how the processing parameters affect the material behavior and how to optimize them.

The optimization of *IEA* related to polymer/carbon fiber composite materials has typically followed a rather Edisonian approach, hindering further development as applications of these materials. Understanding how *IEA* is related to the processing parameters and materials properties is quite challenging, requiring the development of novel methods and models to address the design and property optimization of thermoplastic composites.

Current modeling approaches for predicting crashworthiness of composite structures used in Formula One have been recently assessed by Dallia et al. [10]. Quasi-static and dynamic crush experiments were conducted to generate data for the modeling of a F1 structure. The results showed that crushing efficiency depends on geometry and crushing velocity. The modeling results fit well with data obtained from quasi-static and dynamic experimental tests. The parameters are related just to physical aspects of the Formula One component and the tests velocity, but the processing parameters were not considered on modeling.

Formisano et al. [11] evaluated the influence of the manufacturing parameters on the mechanical behavior of commingled composites. The material was subjected to flexural and impact tests and the results were used to estimate the goodness of fit of a prediction model. The results showed effectiveness of isothermal molding technology compared to the non-isothermal, reducing processing time. The author used glass fiber and polypropylene to manufacture the composites, which differ from the materials tested in this study.

The study of Pascual et al. [12] investigated thermal stability of poly (ether ether ketone) in high temperatures. The consolidation ability of PEEK was verified by thermal analysis. The results indicated morphological changes caused by crosslinking density and crystallinity. In addition, Bernet et al. [13] investigated thermal consolidation of commingled fabrics. A consolidation model was used to investigate different processing techniques as bladder inflation molding and compression–injection molding. Consolidation model assists in determining wire architectures indicating which processing technique to use. Scientific findings are relevant, although processing optimization has not been investigated.

Statistical methods have been used to improve the performance of structural composite materials. Suresh et al. [14] used design of experiments (DOE) method to investigate the effects of processing pressure and coupler concentration on the mechanical behavior of thermoplastic composites. The DOE was based on results of tensile and flexural tests. The study revealed how the processing pressure and the coupler concentration affect the material properties. Lepšík et al. [15] used DOE to optimize the performance of composite tubes according to the angles of the plies and the component geometry. The composite tubes performance was investigated according to the relationship between the ply angles and the specimen lengths for specific loading. None of these works evaluated *IEA* capability of commingled thermoplastic composites.

Singh et al. (2018) [16] conducted studies of recyclability of thermoplastics composites by optimization features. The study was based on polyamide 6 mechanical response on extrusion process to evaluate recyclability and it contributed to define best settings of process parameters. In contribution, Ferreira et al. [17] developed a DOE to identify the effect of microparticles inclusions and stacking sequence on

mechanical properties of hybrid composites. The incorporation of particles improves the mechanical performance of composite materials and can be used to improve the tensile and flexural strength. The influence of the lay-up configuration on in-plane and interlaminar shear properties of composite materials was also investigated by Almeida et al. [18]. Double-notched shear, short beam shear, V-notched rail and Iosipescu shear tests were applied to the composite materials to verify the effects of the lay-up and stacking sequence on the materials performance. The study determined the uniformity of the shear stress state for each test. Our work considered the impact responses of thermoplastic composites and contributes to understanding how the processing parameters affects the material performance.

In recent reports on computational modeling of structural composite materials, Martinez et al. [19] evaluated the fatigue strength behavior of automotive chassis components by artificial neural network (ANN). The study proved that ANN could establish the relationship between the sequence effects and the fatigue life. The influence of different concentrations of fillers and the effects of processing parameters on the wear response of carbon fiber/polyamide composites was studied by Parikh et al. [20]. An ANN was developed to predict the wear response of these materials based on different processing parameters. The study contributes to effectiveness of ANN methodology to optimize the performance of thermoplastic composite materials. Most recently, Di Benedetto et al. (2021) [21] developed an ANN able to predict the energy absorption capability of commingled composites considering the properties of polymer matrix, thermal degradation kinetics and consolidation parameters. However, the effect of each variable on mechanical response was not investigated by any ANN and it need to be more explored.

Here we report the development of a DOE based on an existing factorial design model to relate the processing conditions to the *IEA* of thermoplastic commingled composites. Di Benedetto et al. [22] developed a model which *IEA* of commingled composites is defined according to processing parameters, matrix properties and thermal degradation kinetics. The model was based on LVI tests response of commingled composites. The model can predict *IEA* as a function of temperature and processing time. This study provided an assessment of how pressure, temperature, viscosity, activation energy, impregnation distance, and permeability, or a combination of these variables, affect the mechanical response of the material. In addition, this study contributes to optimization of thermoplastic composites processing.

2. Materials and methods

2.1. Materials processing and characterization

The reinforced fibers were supplied by Toho Tenax. The HTS40 carbon fiber (CF) is characterized by tensile strength of 4240 MPa and elastic modulus of 237 GPa. The polymers yarns were provided by Concordia Manufacturing Co Inc. The specification of the multifilament yarn polyamide 6 (PA6) is Nylon 6–900/72. The 12k CF/PA6 commingled tow has the standard type of interlacing according to the definition of Choi et al. [23]. The specification of the PEEK is PEEK-900/68. The CF/PEEK commingled tow is specified as AS4.

The manufacture of composites structures from commingled thermoplastic yarns requires a heating process directly before the final molding process. In this work, the composite specimens were manufactured by thermoforming, precisely by the hydraulic press Wabash 150–2525–2TMX. The thermal cycle conditions for processing were defined by the thermal degradation analysis and process parameters. Overall, CF/PA6 was manufactured at 240 240 °C, 250 °C, 260 °C, 270° and 280 °C, considering 20 min of soak time with 0.30 MPa (30 t/m²) of pressure. The CF/PEEK was manufactured at 360 °C, 370 °C, 380 °C, 390 °C and 400 °C at the same pressure and soak time mentioned before. More specific details about thermal processing and the mechanical tests performed on these materials can be found in the literature as mentioned before.

Fourier-transform infrared spectroscopy (FTIR) was employed to identify the spectrum of absorption of PA and PEEK, before and after the thermal consolidation. In addition to assessing the purity of these materials, FTIR spectroscopy was also used to verify whether thermal processing affects the chemical structure of the polymers when subjected to high compression rates under molten state. The experiment was performed by Perkin-Elmer Spectrum 100 spectrophotometer with ZnSe conical tip, wavenumber $(1/\lambda)$ range from 650 to 4000 cm $^{-1}$, by attenuated total reflectance method (ATR). The CF/PA and CF/PEEK commingled tows configuration and quality were characterized using scanning electron microscopy (SEM) with a Zeiss EVO15MA microscope.

The constitutive content determination test was carried out according to method I and procedure A of ASTM-D3171; the polymer matrix is chemically removed by acid digestion, allowing the determination of the reinforcement volume. The procedure A indicates the use of nitric acid for PA and PEEK digestion. Five square samples of dimension 20×20 mm of each material were placed in a beaker containing 30 ml of 70% nitric acid in constant mixing at 70 °C for 5 h. The samples were weighed before and after exposure to nitric acid. The reinforcement volume (carbon fiber volume) $\nu_{\rm f}$ is calculated using:

$$v_f = \left(\frac{m_f}{m_i}\right) x 100 x \left(\frac{\rho_c}{\rho_f}\right) \quad , \tag{1}$$

where m_i is the composite initial mass, m_f is the final mass of the composite after acid digestion, ρ_c is the specific mass of the composite and ρ_f is the specific mass of carbon fibers. The specific mass of the composite ρ_c was obtained by method A of ASTM-D792 considering ρ_{water} (at 23 °C)= 0.99 g/cm³, $\rho_{\rm PA}$ = 1.14 g/cm³, and $\rho_{\rm PEEK}$ = 1.32 g/cm³, ρ carbon fiber= 1.78 g/cm³ and described by:

$$\rho_c = \left(\frac{m_s}{m_s - m_u}\right) \rho_{water (23^{\circ}C)} , \qquad (2)$$

where m_s and m_u are, respectively, the dry and wet mass of the composite.

2.2. Thermal degradation of the polymeric matrices

The degradation kinetics is related the degree of degradation α , the time t and a temperature-dependent factor k(T) through the following equation:

$$\frac{d\alpha}{dt} = k(T)f(\alpha) \quad , \tag{3}$$

with k(T) determined by the Arrhenius's equation:

$$\frac{d\alpha}{dt} = A_a e \left(\frac{-E_a}{RT}\right) \quad , \tag{4}$$

where E_a is the reaction activation energy, R is the universal gas constant, and A_a is a pre-exponential factor. For each predetermined degree of degradation α , the Friedman's isoconversional method¹¹ allows the determination of E_a and A_a , considering the degradation degree rate $\frac{d\alpha}{dt}$ as a function of $\frac{1}{a}$, through the relation:

$$ln\left(\frac{d\alpha}{dt}\right) = lnln \quad A_{\alpha} \quad - \quad \frac{E_{\alpha}}{RT} \quad . \tag{5}$$

For each temperature, the Friedman's isoconversional method (Friedman) [24] also allows the determination of the degree of degradation α over time, according to the relation:

$$\alpha = A_a exp\left(\frac{-E_a}{RT}\right)t \quad . \tag{6}$$

The manufacturing of the commingled composites depends on the thermo-oxidative degradation limits. Thermogravimetric methods for

evaluating degradation kinetics of thermoplastic composites are applied considering tests at different heating rates to identify the limits of material degradation, determining E_a a function of α . The peak temperature T_{peak} represents the stage in which the heat input is equal to the heat absorption ratio, following relations:

$$\frac{m(\Delta H)}{gk} = \int_{T_1}^{T_2} \Delta T dT \quad , \tag{7}$$

$$\Delta T_{min} = \left(\frac{dH}{dt}\right)_{min} \frac{m}{gk} \quad , \tag{8}$$

where ΔH is the enthalpy, m is the mass of the material, ΔT is the temperature variation, g and k are constants related to the sample, i.e., the sample port and the instrument used.

Therefore, the degradation time limits for each processing temperature, using a predetermined α , are estimated by the Friedman's isoconversional kinetic method. The polymer melting point T_{melt} is related to the time limit t_{melt} . Finally, the temperature T_{onset} can be determined by thermogravimetry and it is related with the onset-time limit t_{onset} .

2.3. Commingled consolidation parameters

The flow rate of a polymer, u_p , and the impregnation time t_{imp} are determined by the Darcy's law [25] considering the pressure gradient $\frac{dp}{dx}$ = constant. i.e..

$$u_p = -\frac{dx}{dt} = \frac{K}{\nu} - \frac{dP}{dx} \quad , \tag{9}$$

$$t_{imp} = \frac{\nu D_p^2}{2KP} \quad , \tag{10}$$

where K is the permeability coefficient of reinforcing fibers, ν is the polymer viscosity, and D_p is the impregnation distance. D_p is directly related to the polymer yarns distribution throughout the tow. The material compaction during consolidation was obtained empirically by the hydraulic press measurement system used in the material manufacturing. CF/PA6 commingled composite presented 0.3 mm of consolidation degree after processing. The factorial design was used to evaluate the effect of increasing D_p on the impact energy absorption EA.

The use of ultrasound inspections and scanning electron microscopy (SEM) identified the minimum value of P to guarantee the laminate consolidation without defects across the commingled composites cross-section. Similarly, the DOE was able to recognize the effect of P on IEA.

2.4. Multiple regression model for the IEA

The multiple regression model employed to generate the DOE analysis that relates the impact energy absorption *IEA* to the materials properties and processing conditions was obtained in a recent work of Di Benedetto et al. [22], and can be written as follows:

$$IEA = \beta_0 + \beta_1 \left(\frac{-E_a}{\ln\left(\frac{a}{A_a}t\right)} \right) + \beta_2 \left(\frac{\nu D_p^2}{2KP} \right), \tag{11}$$

where β_0 , β_1 , and β_2 are the regression coefficients. This analytical model combines the degradation limits with the consolidation parameters to predict the *IEA* capability of commingled composites; it considers the matrix degradation caused by the increase in temperature, the matrix properties, the processing parameters, and the thermal degradation kinetics. The multiple regression statistical analysis was conducted by the open-source software Rstudio. The regression model is based on a well-established least squares method and stepwise method. According to Agostinelli [26], the stepwise method of variable selection

determined a subset of independent variables that best explains the response. This study introduced robust stepwise regression procedures to improve the effectiveness of regression models.

2.5. Statistical experiments

The data acquisition by the test matrix contains n=64297 observations. The factorial design was created using full resolution and 2-level factorial with 4 design factors (independent variables) to create a model design. The response of the custom factorial design was the *IEA* of the commingled composites. The factorial design analysis was performed using Minitab.

DOE is a statistical tool used to verify and analyze the effect of the processing parameters, polymeric matrix properties, and the thermal degradation kinetics, on the *IEA*. The residual data analysis also reveals information about the behavior of the material when processed using different consolidation parameters and matrix properties. Regardless of the purpose of the DOE analysis is to evaluate the effects of factors over *IEA* capability, it was extremely important to distinguish the changes in response caused by the residual variability.

The independent variables of the factorial design model were determined according to Eq. (8), which relates the independent variables and constants of the thermal consolidation process. Since the regression model developed previously was based on the CF/PA6 commingled composite response in the LVI test, the *IEA* was considered as the dependent variable. Other factors of Eq. (8) were assumed constants of the analytical analysis. Table 1 summarizes the factors and their range and intervals of values used in the DOE analysis.

The range of values of the independent variables were obtained according to the empirical tests with CF/PA6 commingled composite. Thereby, the processing parameters such as temperature and pressure were used considering the thermal consolidation conditions applied to the material. The impregnation distance (D_p) depends on the homogeneity of the distribution of the polymer yarn along the reinforced 12k carbon tow. $D_p = 0.3$ mm is the minimum value that provides the impregnation and wetting of the reinforcing fibers by the polymeric matrix in the molten state. Total elimination of the material voids occurs from this value.

Table 1 Limiting values or ranges for each factor entering Eq. (1) used to generate the DOE analysis.

Factor		Unit	Value/ Range	Interval
Independent	Temperature, T_p	°C	250-390	1
Variables	Pressure, P	Pa	300-390	5
	Viscosity, ν	Pa.s	1000-2000	200
	Impregnation	mm	0.3-1.2	0.3
	Distance, D_p			
Constants	Activation Energy, E_a	J/mol	93699.03	_
	Gas Constant, R	$J.mol^{-1}$. K^{-1}	8.314	-
	Degree of	_	0.05	_
	Degradation, α			
	Pre-Exponential	s^{-1}	31708.22	_
	Factor, A_{α}			
	Time, t	S	1200	_
	Permeability, K	m^2	1.40E-10	_
	Regression	_	80.021	_
	coefficient, β_0			
	Regression	_	-0.179	-
	coefficient, β_1			
	Regression coefficient, β_2	-	-0.067	-

3. Results and discussion

3.1. Spectroscopic analysis and chemical compositions

The FTIR absorption spectra of PEEK and PA are shown in Fig. 1(a) and (b). The characteristic peaks of transmittance are associated with vibration frequencies of the functional groups of each molecular structure. According to the FTIR results, no changes in the chemical structure composition of the materials were observed due to the thermal consolidation process. The same characteristic peaks were observed after and before consolidation, as evidenced by the perfect overlapping of the spectra. In addition, the IR spectra of PEEK and PA indicate the absence of impurities and contaminants in their chemical structure.

The IR spectra of PEEK presented characteristic peaks associated with stretch vibration frequencies of C-H (\sim 3000 cm $^{-1}$), ketone ring (\sim 1700 cm $^{-1}$) and ether group (-O- at \sim 1100 cm $^{-1}$). The polyamide spectra exhibit the characteristic absorption peaks associated with the ketone (C=O at 1635 cm $^{-1}$), Amide II (N-H at 3296;1534 cm $^{-1}$) and C-H (3075–2863; 1462–1417 cm $^{-1}$) groups (Ma et al.) [27]. The observed equivalence of intensity between the amide and hydrocarbon groups indicates that the polyamide 6 was used in the CF/PA commingled tow.

3.2. Commingled tow microscopy

Micrographs of CF/PEEK commingled tow of 7 μm diameter and PEEK yarn of 26 μm diameter are shown in Fig. 2(a) and (b), respectively. Similarly, CF/PA commingled tow microscopic analysis is shown in Fig. 3(a) and (b). It reveals a multifilament PA yarn with 37 μm diameter and carbon fiber with 7 μm diameter. From these results, the heterogeneity of distribution between the fibers and yarns along the commingled tow is in evidence and requires a more in-depth assessment as revealed by microscopy.

The distribution of carbon fiber and polymer yarns within the commingled tow were studied with SEM, the results of which are shown in Fig. 4(a). The cross-section SEM image revealed regions of high fiber concentration (Region I) and high concentration of polymer yarns (Region II). Fig. 4(b) is a binary image of (a) to emphasize the differences between the regions I and II, in which the carbon fiber cross-section is represented by black dots and polymer yarns cross-section is represented by black spots.

Although heterogeneity was observed in the tow, different distribution patterns were identified in the same cross-section of the commingled tows. These were classified in three general patterns (I, II and III) shown with schematics in Fig. 5. Pattern I is described by the most homogeneous distribution type of a commingled tow. The sections which present this pattern type favor the wettability of the molten polymer during thermal consolidation process. This phenomenon occurs due to the reduction of the impregnation distance, which is related to the distance covered by the viscous flow when the pressure is applied. The direction of the viscous flow is random and the impregnation distance \mathcal{D}_p is reduced (see Eq. 10). Differently, Pattern II presents a concentric viscous flow direction, and Pattern III presents unidirectional viscous flow. The distance \mathcal{D}_p , required to impregnate the reinforcement fibers during consolidation, is higher for the Pattern II and III in comparison to the Pattern I.

3.3. Acid digestion

For evaluating the reinforcement fiber content, we employed acid digestion according to method I proposed by the ASTM-D3171 standard, which is considered the most applied and representative method for determining the reinforcement fiber content in composite materials. The results are summarized in Table 2. We find that CF/PA presents 53.87% of reinforcement fiber volume, while CF/PEEK presents 50.12% of reinforcement fiber volume. These values are compatible with structural composite materials constitutive content fraction.

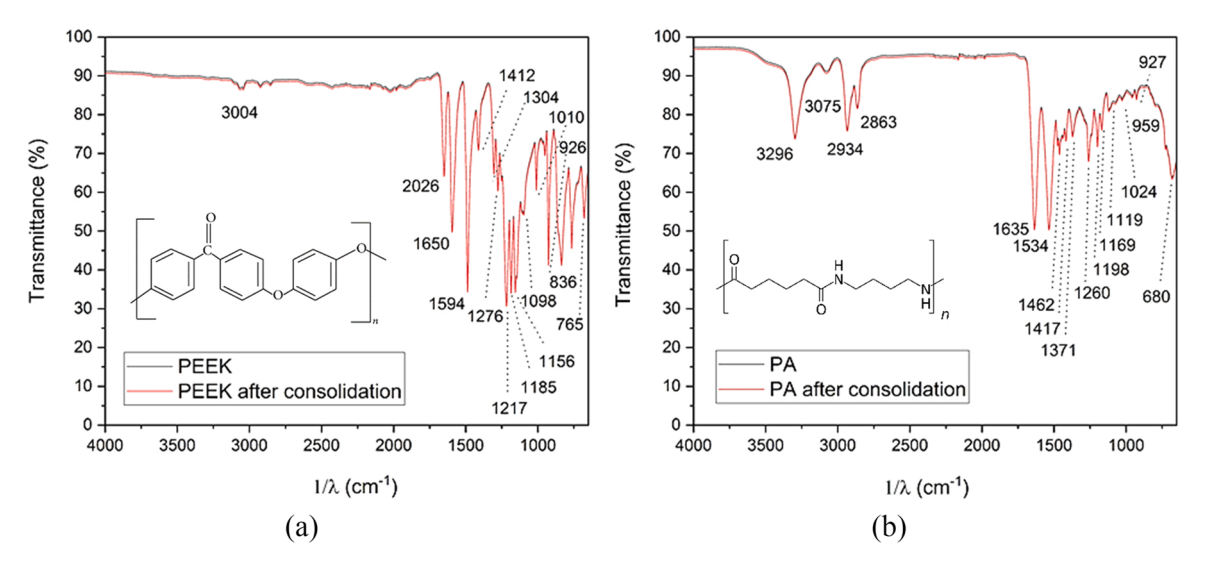


Fig. 1. FTIR spectra of (a) PEEK and (b) PA vibration characteristics of the respective functional groups, indicating that the material chemical structure composition remains unchanged before and after the thermal consolidation process.

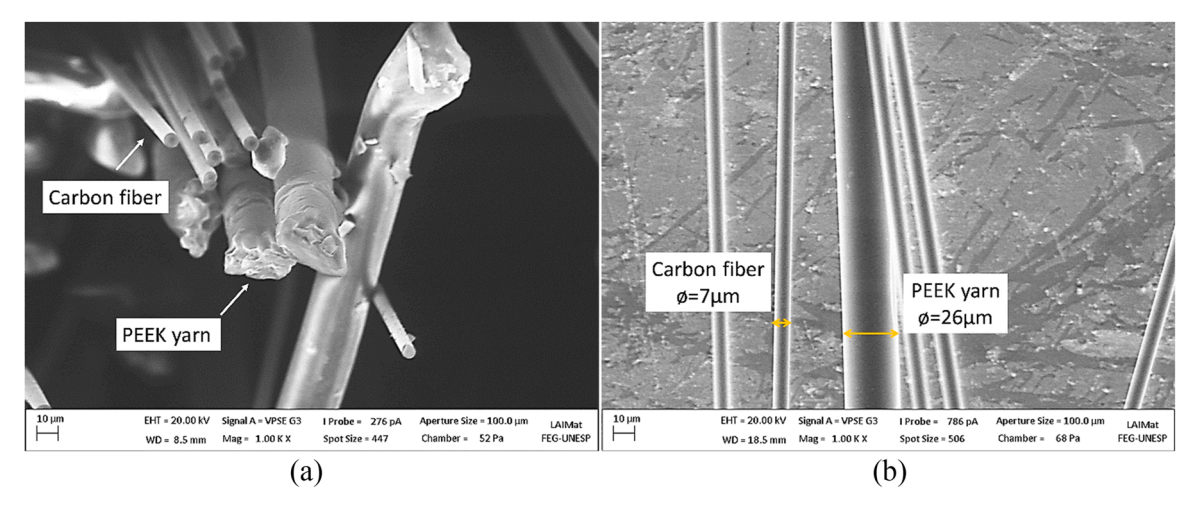


Fig. 2. CF/PEEK commingled tow constituent evaluation by SEM according to Di Benedetto et al. . Details of the carbon fiber and PEEK yarn are shown in (a) and the, and the diameter measurements are indicated in (b).

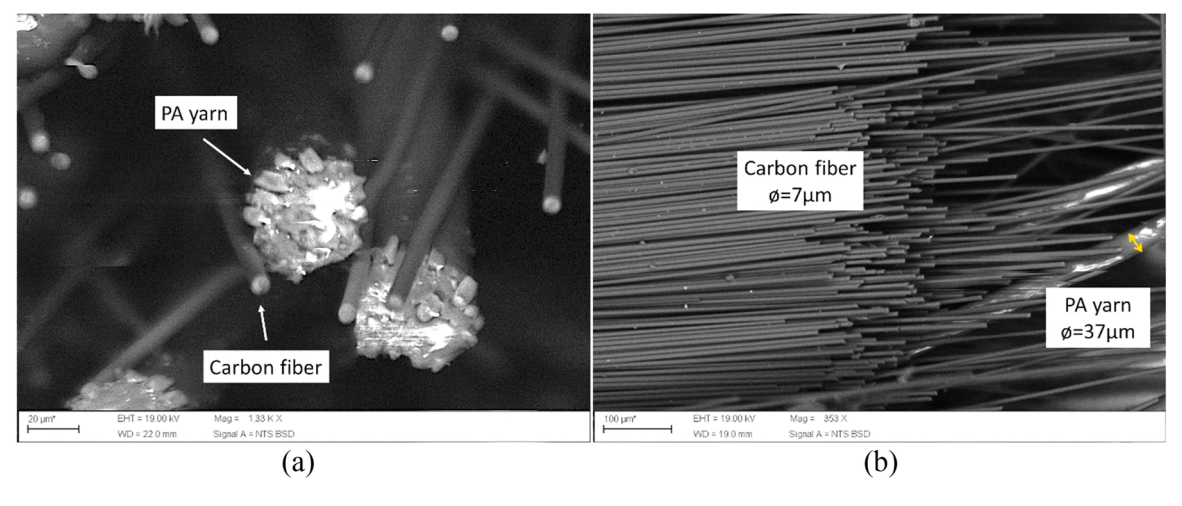


Fig. 3. CF/PA commingled tow constituent evaluation by SEM as revealed by Di Benedetto et al. . (a) Details of the carbon fiber and PA yarn are shown in (a), and the diameter measurements are indicated in (b).

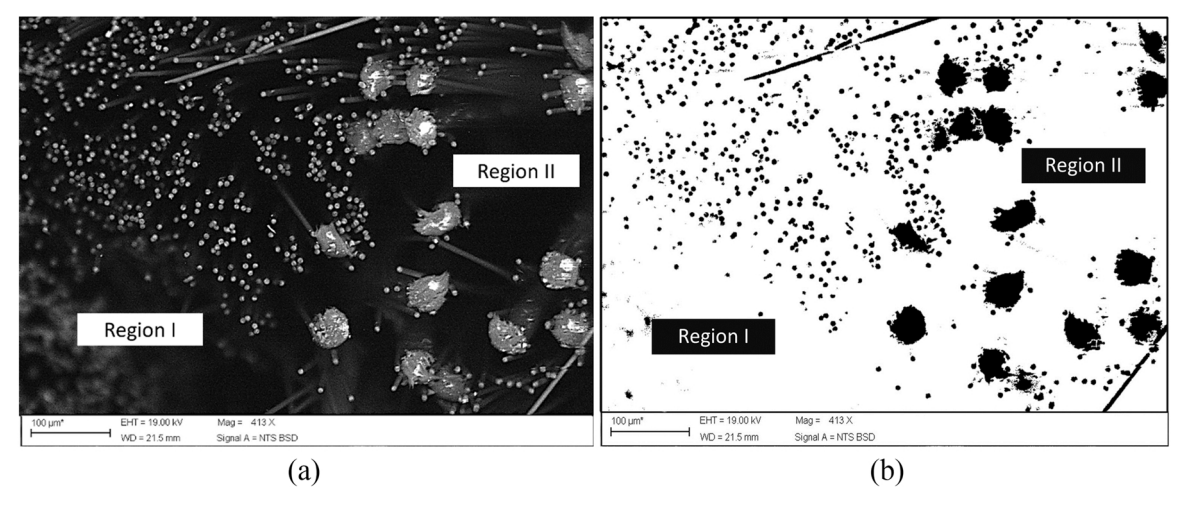


Fig. 4. SEM image of the distribution of the reinforced fiber and polymer yarns within the commingled tow. (a) Cross-section of the commingled tow as revealed by Di Benedetto et al. . (b) Binary image detailing the distribution; black dots represent the carbon fiber cross-section and black slots represent the polymer yarn cross-section.

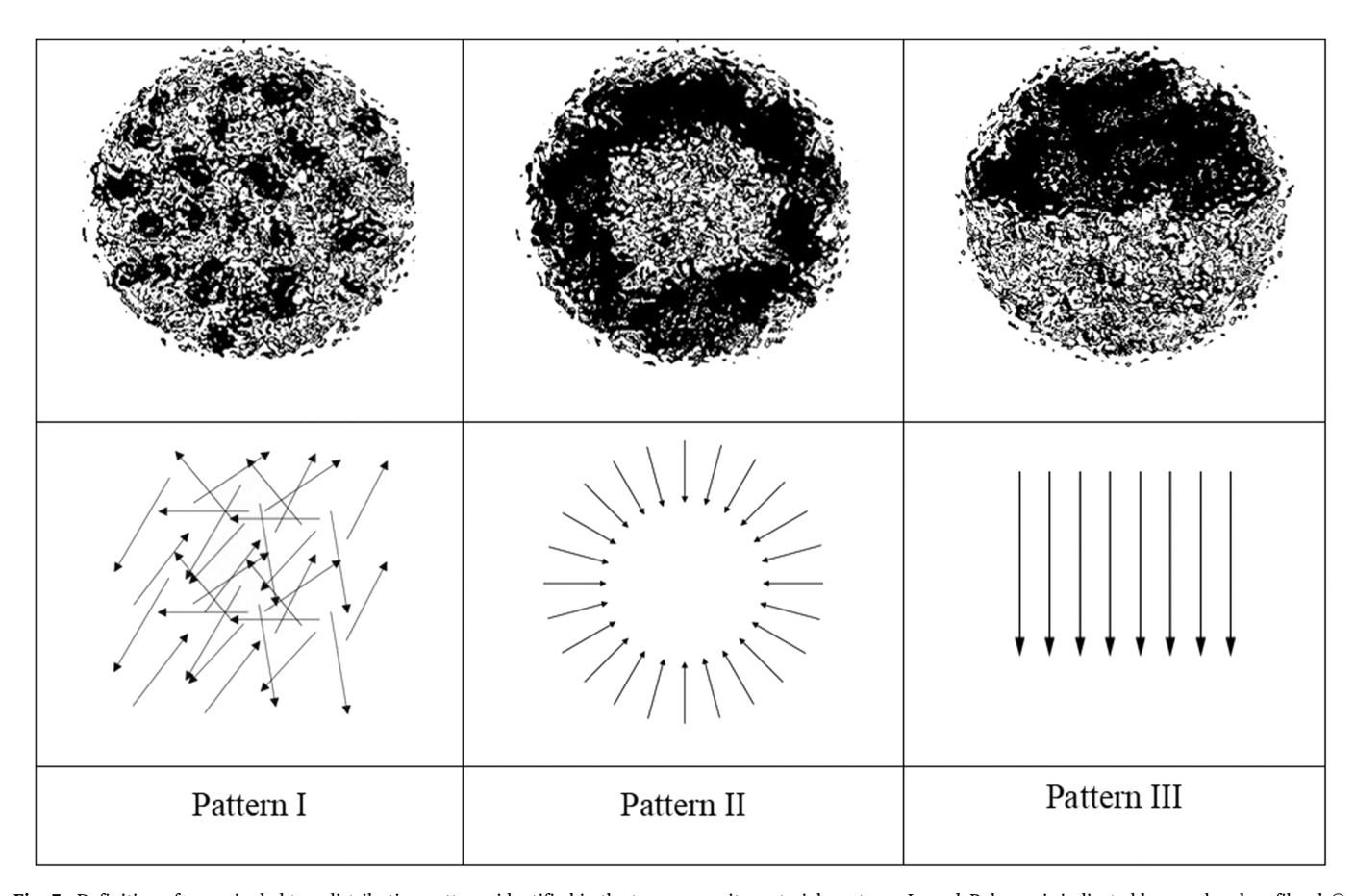


Fig. 5. Definition of commingled tow distribution patterns identified in the two composite materials systems. *Legend*: Polymer is indicated by ● and carbon fiber by Direction of the matrix viscous flow during consolidation are indicated by arrows (↑) in the bottom panels.

3.4. Friedman's isoconversional method

Friedman's isoconversional method allowed the prediction of the degree of degradation as a function of time and temperature of the processing. Moreover, graphical plots determined the process window of each material. The kinetics parameters of the thermal degradation analysis, such as temperature, time, activation energy and molecular mass, based on the Friedman's method, for both PA and PEEK, are listed

in Table 3. Fig. 6 is the graphical result of the degradation kinetics analysis for the CF/PA commingled composite. It reveals the relation between the activation energy E_a and α in (a) and the limits of degradation according to T_p in (b). Fig. 7 shows the degradation kinetics analysis of the CF/PEEK commingled composite.

 Table 2

 Summary of measurements to reinforcement fiber volume determination.

Material	Sample	Dry mass (g)	Wet mass (g)	m _{initial} (g)	m _{final} (g)	$\rho_{\rm c}~({\rm g/cm}^3)$	Reinforcen	nent volume (%)
CF/PA	1	0.6297	0.1960	5.0100	3.3040	1.44	53.26	53.87
	2	0.6341	0.1992	5.3990	3.5730	1.44	53.67	
	3	0.6098	0.1870	5.0440	3.4380	1.43	54.68	
CF/PEEK	1	0.6997	0.1890	5.0010	3.2950	1.36	50.21	50.12
	2	0.7042	0.1922	5.0020	3.2900	1.36	50.31	
	3	0.6798	0.1800	5.0100	3.3010	1.35	49.84	

 $\begin{tabular}{ll} \textbf{Table 3} \\ \textbf{Thermal degradation kinetics parameters obtained by Friedmann's isoconversional method.} \end{tabular}$

Material	Temperature,		Time, t		Ea ($\alpha = 0.05$)	Molecular Mass
	T (°C)		(min)		kJ/mol	(g/mol)
	melt	onset	melt	onset		
PA	220	320	112	4.5	93.70	113
PEEK	338	550	142	12.3	73.26	228

3.5. Results of the factorial design method

The absolute values of the standardized effects are shown in a Pareto chart in Fig. 8. The standardized effects are t-statistics that test the null hypothesis ($H_0 =$ null effect) and they are classified from the largest effect to the smallest effect. Also, the Pareto chart displays a reference line (t_{calc} =2) to indicate which effects are statistically significant based on the significance level α assumed. t_{calc} depends on the value of α assumed and the number of degrees of freedom.

The impregnation distance D_p and temperature T are the independent variables that cause greater effect over $I\!E\!A$. The matrix viscosity ν

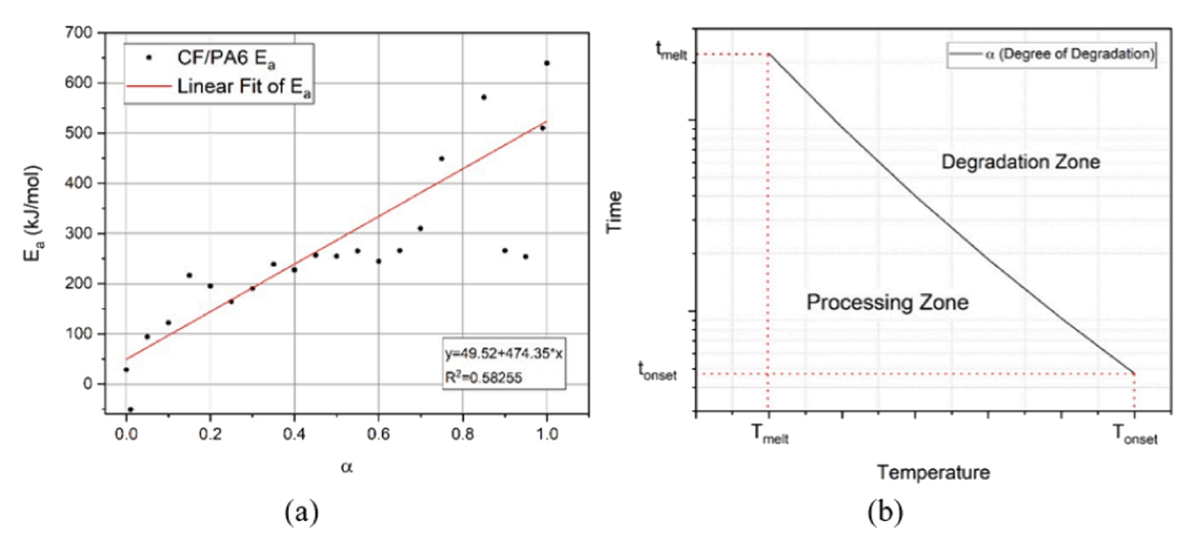


Fig. 6. Thermal degradation kinetics analysis for CF/PEEK. (a) E_a versus α . (b) Thermal degradation limits plot.

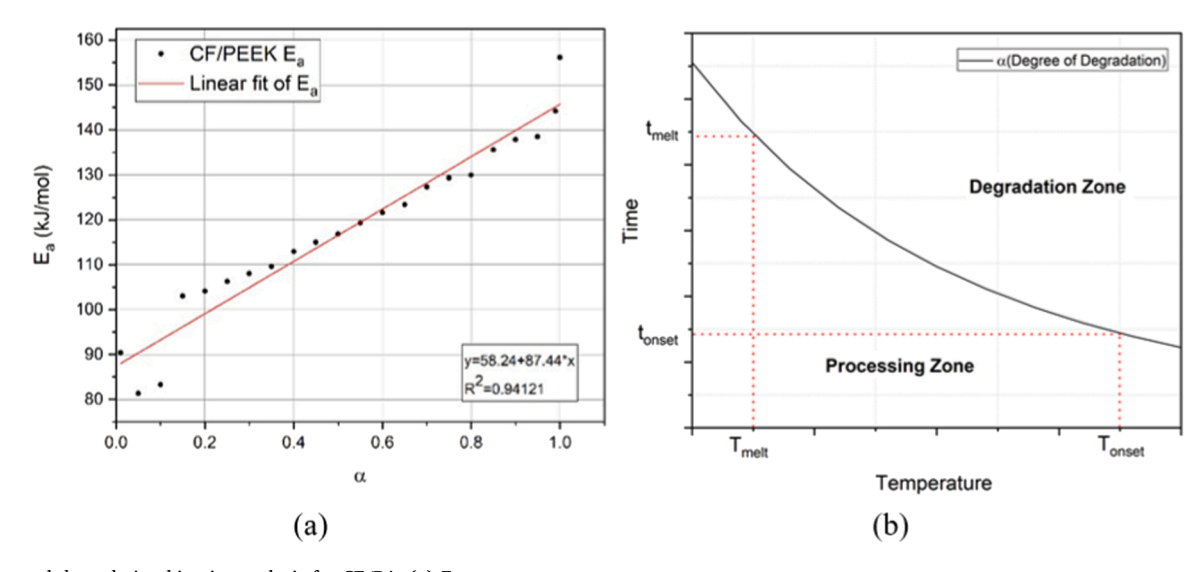


Fig. 7. Thermal degradation kinetics analysis for CF/PA. (a) E_a versus α . (b) Thermal degradation limits plot adapted from Di Benedetto et al.

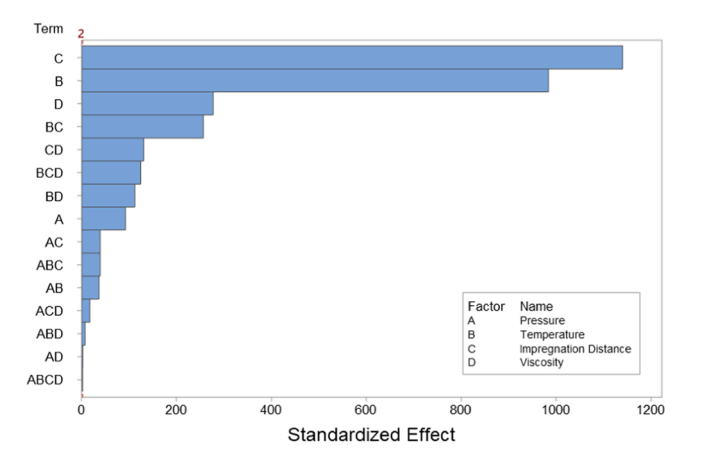


Fig. 8. Pareto chart of the standardized effects on *IEA* revealing the level of the effects and its interaction.

and the interaction between processing temperature T_p and impregnation distance D_p have similar effects on *IEA*. Next, the consolidation pressure P had less effect compared to the other independent variables of the test matrix. As an exception, the interaction between all these four parameters had no significant effect on *IEA*.

Because the Pareto chart only displays the absolute value of the effects, it is not possible to determine which processing and materials parameters lead to an increase or decrease in *IEA*. For this reason, using the normal probability plot of the standard effects in Fig. 9 helps to examining how these parameters affect the *IEA*, both in magnitude and direction.

The increase in the temperature T_p , impregnation distance D_p , and viscosity ν affects negatively (reduction) the IEA. The difficulty associated with the permeation of the molten matrix in the reinforcement fibers causes an increase in D_p , especially in cases of heterogeneity in the distribution of yarns and fibers in the commingled tow. The negative effect on IEA by the increase in D_p is related to the increased time required for fiber wettability (also polymer relaxation), which contributes to matrix degradation. The increase in the pressure P has a positive effect on IEA due to material consolidation rate and fiber wettability by the molten matrix. And, finally, lower viscosity values make the consolidation process more efficient and increase the mechanical strength of the laminate.

The magnitude of the effects is different for each factor; the steeper slope of the line in Fig. 9, the greater magnitude of the effect. Note that the plot of the main effect in Fig. 9 does not reveal the interactions

between processing and materials parameters, so the use of an interaction plot, shown in Fig. 10, is required. This interaction plot shows how the relationship between one categorical factor (or parameter) and *IEA* depends on the value of the second categorical factor.

By assessing the plot lines in Fig. 10, one can understand how interactions affect the relationship between factors and response. The combined pairs T_p and D_p , D_p and ν , and T and ν presents the highest level of interaction effect on *IEA*. Although non-negligible, the interaction between the other pairs of factors is of much lesser magnitude. Only interactions involving the pressure P have a positive effect on *IEA*, i.e., increase the *IEA* capability of the material.

The overall results of the analysis of variance are shown in Table 4, where the importance of each factor is listed. It can be noted that all factors are significant and only one interaction, namely $P*T*Dp*\nu$, was found to have no significance (p-value = 0.068).

The adjusted R-squared (R-sq adj), which compares the explanatory power of the regression model that contains different numbers of predictors, is 97.46%, demonstrating the reliability of our factorial regression model. The results of the regression model develop by Di Benedetto et al. (2021) [21] are listed in Table 5.

Next, the results of the study of residuals from the factorial experiment reveal the difference between the actual and predicted values of the design model. The result of the Anderson-Darling normality test reveals a calculated p-value lower than the significance level α , implying the rejection of the null hypothesis of normality of the distribution of residues, despite the similarity of the histogram with a Gaussian curve. Non-observance of a pattern or trend on the Fit and Order charts indicates that the external influences affecting the experimental results have been minimized.

The interpretation of the residual analysis of the DOE implies a situation where the random disturbance in the relationship between the independent variables and the dependent variable is different in all values of the independent variables. This phenomenon is associated with heteroscedasticity, which is a systematic change in the propagation of residual errors over the range of measured values.

In summary, the heteroscedasticity observed refers to the circumstance in which the variability of a variable is unequal across the range of values of a second variable that predicts it. In this particular study, heteroscedasticity means that the energy absorption capability of commingled composites depends on the processing parameters, matrix properties and degradation kinetics, but the response prediction varies with each combination of these factors. This fact indicates that the thermal consolidation must be carefully studied to optimize the *IEA* capability and the composite component crashworthiness, increasing the component reliability and human safety in an eventual automotive

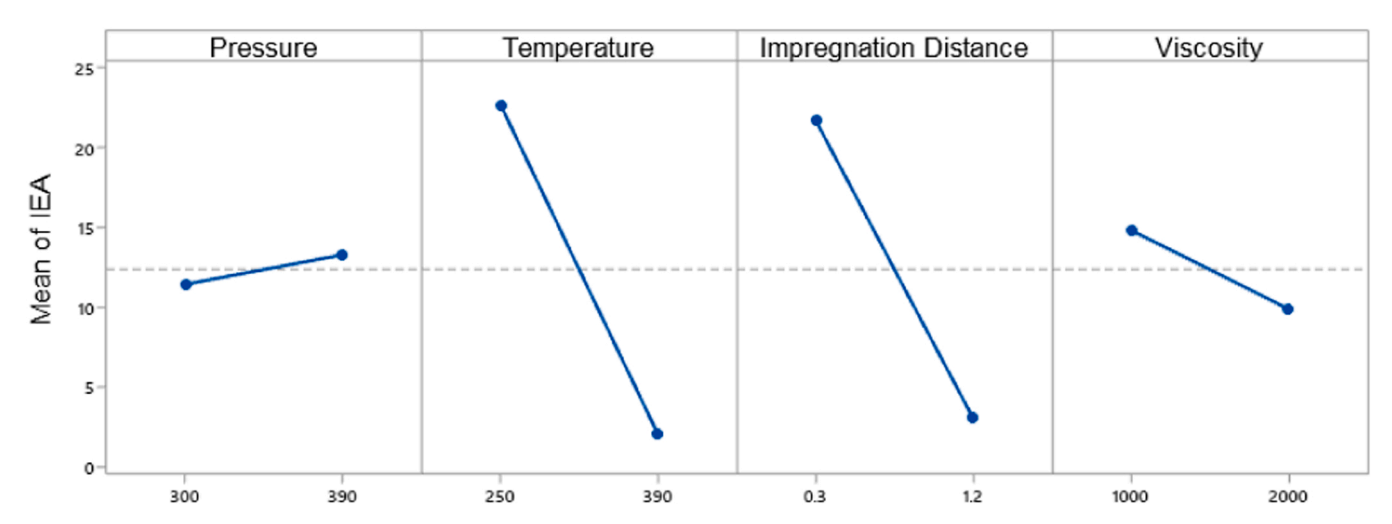


Fig. 9. Variation of *IEA* as function of the main processing and materials parameters P, T_p , D_p and ν , considering their lower and upper limits.

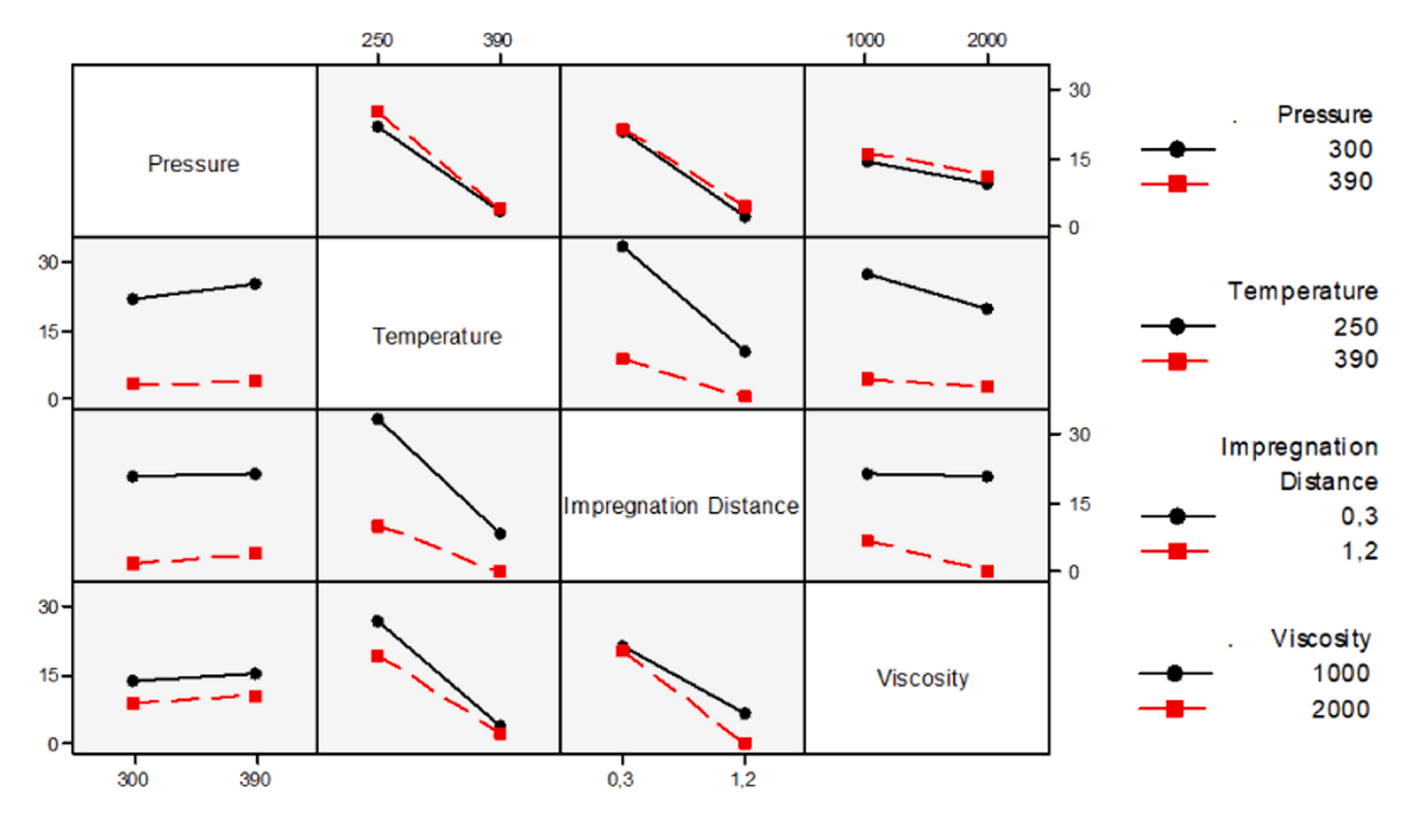


Fig. 10. Plot of interaction factors for IEA, showing how the variables are combined creating interaction.

Table 4 Coded coefficients of factorial regression.

Term	Effect	Coef	SE Coef	T-Value	P-Value
Constant		12.3754	0.0061	2031.39	0.0000
P	1.8448	0.9224	0.0100	92.14	0.0000
T	-20.6263	-10.3132	0.0105	-984.33	0.0000
Dp	-18.6447	-9.3223	0.0082	-1140.57	0.0000
ν	-4.9377	-2.4689	0.0089	-276.84	0.0000
P * T	-1.2514	-0.6257	0.0172	-36.34	0.0000
P * Dp	1.0457	0.5228	0.0134	38.93	0.0000
P * ν	-0.0606	-0.0303	0.0147	-2.07	0.0390
T * Dp	7.2002	3.6001	0.0141	256.11	0.0000
Τ * ν	3.4306	1.7153	0.0153	111.84	0.0000
Dp* ν	-3.1231	-1.5616	0.0120	-130.51	0.0000
P * T * Dp	-1.7864	-0.8932	0.0231	-38.67	0.0000
P * T * ν	-0.3530	-0.1765	0.0252	-7.00	0.0000
P * Dp* ν	-0.6644	-0.3322	0.0197	-16.90	0.0000
T * Dp* ν	5.1128	2.5564	0.0206	124.24	0.0000
P * T * Dp* ν	-0.1235	-0.0618	0.0338	-1.83	0.0680

Table 5Power analysis of the regression model from Di Benedetto et al. (2021).

S	R-sq	R-sq (adj)	R-sq (pred)
1.54476	97.46%	97.46%	97.46%

collision.

A practical effect of heteroscedasticity on *IEA* can be seen by Fig. 11. The surface response of the regression model was applied considering a reduction of the impregnation distance. It is noticeable that the behavior of the material is different according to the combination of factors temperature T_p , pressure P and impregnation distance D_p .

At each combination of T_p , P and D_p , an unparalleled response plan is observed. It means that the material's response in absorbing impact energy is different for each combination of factors related to the thermal consolidation process.

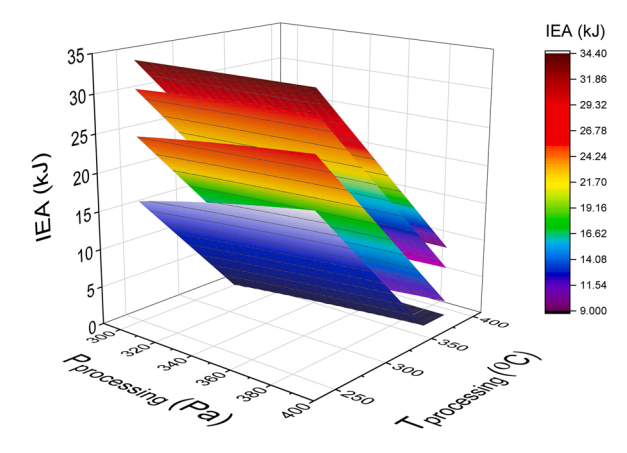


Fig. 11. Representative 3D response surface considering the increase of impregnation distance \mathcal{D}_{v} .

Although the factorial analysis presents, in its entirety, heteroscedasticity, there are cases in which the variance of residual errors is statistically equal, revealing a punctual homoscedasticity. Fig. 12 is a 3D surface response of *IEA* considering the increase of the matrix viscosity.

The response optimizer feature for the factorial design has identified the combination of input variable settings that optimize the *IEA* response. Therefore, the combination P=390 Pa, $T_p=250\,^{\circ}$ C, $D_p=0.3$ mm and $\nu=2000$ Pa.s provides the maximum *IEA* value (36.09 kJ), according to the response optimization chart. However, note that the determination of the optimum process parameters also depends on other factors such as production cost, productivity, machinery capability, matrix type and thermal degradation kinetics properties of each composite material.

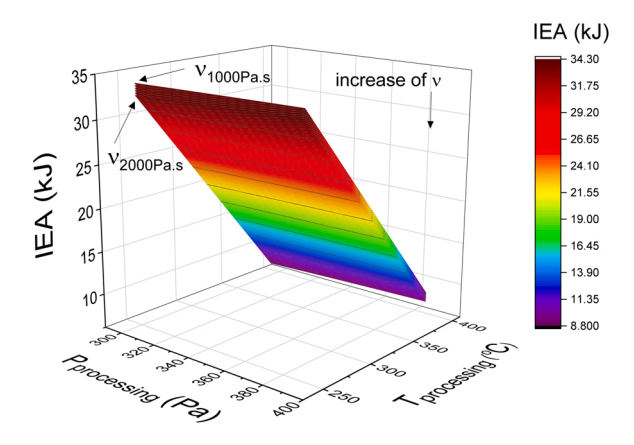


Fig. 12. Representative 3D surface response considering the increase of viscosity ν .

4. Conclusions

A statistical analysis was used to quantify the causal relationship between the processing parameters and the mechanical behavior of thermoplastic commingled composites. The results indicate a path to improving the capability to absorb impact energy and, thus, increase crashworthiness by relating it to thermal degradation kinetics, polymeric matrix properties, and processing parameters. In particular, we find that the material crashworthiness strongly depends on the degradation kinetics, making the material more resistant to an impact event when the degradation rates are reduced. The matrix viscosity also affects the IEA capability of commingled composites; it is related with the impregnation distance D_p and wettability of the reinforced fibers on tow during consolidation. Three different types of polymer/fiber distribution were observed, with distinct values of D_p . The most homogeneous polymer/fiber distribution (Pattern I) facilitates the fiber impregnation by the molten state matrix, related to the shortest D_p , gives largest *IEA*. Our results show that the combination of Darcy's law and Friedman's isoconversional method is a powerful tool to optimizing the performance of thermoplastic composite materials for application in automotive component, relating it to the variables of the manufacturing process.

Declaration of Competing Interest

The authors declare that they have no known competing financial interests or personal relationships that could have appeared to influence the work reported in this paper.

Acknowledgments

This works was supported by the FAPESP, grant numbers 2019/22173-0, 2018/24964-2 and 2017/16970-0, from the CNPq, grant numbers 303224/2016-9 and 311709/2017-6, from FINEP, grant number 0.1.13.0169.00, and FAPEMIG grant number APQ-00385-18 and APQ-01846-18. AJ acknowledges support from NSF Early Career Award, grant number DMR-1652994.

References

[1] R.M. Di Benedetto, A.J. Janotti, G.F. Gomes, A.C. Ancelotti Junior, E.C. Botelho, Development of hybrid steel-commingled composites cf/peek/bwm by filament

- winding and thermoforming, Compos. Sci. Technol. 218 (2022) 1–20, https://doi.org/10.1016/j.compscitech.2021.109174.
- [2] S.J. Pety, J.E. Aw, A.C. Gendusa, P.R. Barnett, Q.A. Calvert, N.R. Sottos, S.R. White, Effect of microchannels on the crashworthiness of fiber-reinforced composites, Compos Struct 184 (2018) 428–436.
- [3] D.M. Garner, D.O. Adams, Test methods for composites crashworthiness: a review, J. Adv. Mater. 40 (2008) 5–26.
- [4] Z. Zhang, W. Sun, Y. Zhao, S. Hou, Crashworthiness of different composite tubes by experiments and simulations, Compos. Part B Eng. 143 (2018) 86–95.
- [5] E. Korich, G. Belingardi, A. Tekalign, D. Roncato, B. Martorana, Crashworthiness Analysis of Composite and Thermoplastic Foam Structure for Automotive Bumper Subsystem. Adv. Compos. Mater. Automot. Appl. Struct. Integr. Crashworthiness, John Wiley & Son, 2014, pp. 129–147.
- [6] R.M. Di Benedetto, O.A. Raponi, D.M. Junqueira, A.C. Ancelotti Junior, Crashworthiness and Impact Energy Absorption Study Considering the CF/PA Commingled Composite Processing Optimization, Mater Res 20 (2017) 792–799.
- [7] P. Parina, R. Hull, R.W. Mccabe, D. Flath, J. Grasmeder, M. Percy, Mechanism of thermal decomposition of poly(ether ether ketone) (PEEK) from a review of decomposition studies, Polym. Degrad. Stab. 95 (2010) 709–718.
- [8] Y. Ren, H. Jiang, B. Gao, J. Xiang, A progressive intraply material deterioration and delamination based failure model for the crashworthiness of fabric composite corrugated beam: Parameter sensitivity analysis, Compos. Part B Eng. 135 (2017) 49–71.
- [9] P.H. Thornton, Energy absorption in composite structures, Compos. Mater 13 (1979) 247.
- [10] D. Dallia, L.F. Varandas, G. Catalanotti, S. Foster, B.G. Falzon, Assessing the current modelling approach for predicting the crashworthiness of Formula One composite structures, Compos. Part B Eng. 2015 (2020) 1–19.
- [11] A. Formisano, I. Papa, V. Lopresto, A. Langella, Influence of the manufacturing technology on impact and flexural properties of GF/PP commingled twill fabric laminates, J. Mater. Process. Technol. 274 (2019) 1–5.
- [12] A. Pascual, M. Toma, P. Tsotra, M.C. Grob, On the stability of PEEK for short processing cycles at high temperatures and oxygen-containing atmosphere, Polym. Degrad. Stab. 165 (2019) 161–169.
- [13] E. Babakus, C.E. Ferguson, K.G. Joreskog, The sensitivity of confirmatory maximum likelihood factor analysis to violations of measurement scale and distribution assumptions, J. Mark. Res. 24 (1987) 222–228.
- [14] S. Suresh, V.S.S. Kumar, Experimental determination of the mechanical behavior of glass fiber reinforced polypropylene composites. GCMM (2014) 632–641.
- [15] Lepšík, P., Kulhavý P. Design optimization of composite parts using doe methoD. 58th ICMD 2017, 2017, pp. 200–205.
- [16] R. Singh, R. Kumar, N. Ranjan, R. Penna, F. Fraternali, On the recyclability of polyamide for sustainable composite structures in civil engineering, Compos. Struct. 184 (2018) 704–713.
- [17] B.T. Ferreira, L.J. Silva, T.H. Panzera, J.C. Santos, R.T. Santos, F. Scarpa, Sisal-glass hybrid composites reinforced with silica microparticles, Polym. Test 74 (2019) 57–62.
- [18] J.H.S. Almeida, C.C. Angrizani, E.C. Botelho, S. Amico, Effect of fiber orientation on the shear behavior of glass fiber/epoxy composites, Mater. Des. 65 (2015) 789–795.
- [19] M.J. Martinez, M.A. Ponce, Fatigue damage effect approach by artificial neural network. Int. J. Fatigue 124 (2019) 42–47.
- [20] Parikh, H.H., Gohil P.P. Experimental determination of tribo behavior of fiber-reinforced composites and its prediction with artificial neural networks. Durab. Life Predict. Biocomposites, Fibre-Reinforced Compos. Hybrid Compos., 2019, pp. 301–320.
- [21] R.M. Di Benedetto, E.C. Botelho, A. Janotti, A.C. Ancelotti Junior, G.F. Gomes, Development of an artificial neural network for predicting energy absorption capability of thermoplastic commingled composites, Compos. Struct. 257 (2021) 113-131
- [22] R.M. Di Benedetto, E.C. Botelho, G.F. Gomes, D.M. Junqueira, A.C. Ancelotti Junior, Impact energy absorption capability of thermoplastic commingled composites, Compos. Part B Eng. 176 (2019) 1–29.
- [23] Choi, B.D., Diestel, O., Offermann P. Commingled CF/PEEK Hybrid Yarns for Use in Textile Reinforced High Performance Rotors. 12th Int. Conf. Compos. Mater., 1999, pp. 1–10.
- [24] H.L. Friedman, Kinetics of thermal degradation of char-forming plastics from thermogravimetry, J. Polym. Sci. Polym. Symp. 6 (1964) 183–195.
- [25] A.M. Sastry, Impregnation and consolidation phenomena, Compr. Compos. Mater. 2 (2000) 609–622.
- [26] C. Agostinelli, Robust stepwise regression, J. Appl. Stat. 29 (2002) 9–16.
- [27] Y. Ma, U. Masahito, T. Yokozeki, T. Sugahara, Y. Yang, H. Hiroyuki, Investigation of the flexural properties and failure behavior of unidirectional CF/Nylon 6 and CF/Epoxy composites, J. Compos. Mate.r 7 (2017) 227–249.